



PII S0016-7037(99)00092-7

Re-Os isotope and Pd/Ru variations in chromitites from the Critical Zone, Bushveld Complex, South Africa

TOM E. McCANDLESS,^{1,*} JOAQUIN RUIZ,¹ B. IVAN ADAIR,^{†,2} and CLAIRE FREYDIER¹¹ Center for Mineral Resources, Department of Geosciences, University of Arizona, Tucson, AZ 85721, USA² CSIRO, Box 883 Kenmore, Queensland, Australia 4069

(Received August 17, 1998; accepted in revised form February 9, 1999)

Abstract—Rhenium-osmium isotope measurements of selected chromitites from the Critical Zone of the Bushveld igneous complex reveal that a significant component of radiogenic Os was present in the magma when it formed 2.06 Ga ago. Measured $^{187}\text{Os}/^{188}\text{Os}$ ratios increase with stratigraphic height, and individual layers have similar values across the complex. Initial $^{187}\text{Os}/^{188}\text{Os}$ ratios for chromitites from the western Bushveld decrease from 0.140 at the LG to 0.129 at the MG2 chromitite, increasing to 0.153 at the UG2 chromitite. The inflection at MG2/MG3 is the boundary between the lower and upper Critical Zone, consistent with previous mineralogical and geochemical studies indicating a shift in magma composition at this point. Chromite separates have γOs values of $\sim 12\text{--}35$ at 2.06 Ga and are too radiogenic for a purely mantle derivation. Assimilation of 5% mafic granulitic lower crust in a tholeiitic parent magma can explain the radiogenic values. Pd/Ru ratios for the intergranular and chromite separate components of each layer differ by orders of magnitude, but relative shifts from layer to layer are similar. Combined with the Re-Os data, the results suggest that PGE were concentrated into chromitites by magmatic or early deuteric processes that were specific to each layer. Post-layering, upward mobilization of PGE by hydrothermal processes probably did not play a significant role in PGE enrichment. Copyright © 1999 Elsevier Science Ltd

1. INTRODUCTION

Covering an area of over 60,000 square kilometers, the Bushveld is one of the largest igneous complexes in the world. The Rustenburg Layered Suite that comprises the igneous stratigraphy can be correlated in outcrops over 300 kilometers apart, and with an estimated volume of more than 380,000 cubic kilometers (Cawthorn and Walraven, 1997), is larger than some continental flood basalt provinces (Hooper, 1988). The Bushveld Complex also accounts for about 40% of world platinum-group element (PGE) production, and is many times larger than the Stillwater or Great Dyke PGE deposits (Willemse, 1969; Loebenstein, 1984).

A large number of field, mineralogical and isotopic studies have elucidated the igneous processes responsible for the formation of the Bushveld, and for its unique enrichment in platinum group elements (Kinloch, 1982; Kruger and Marsh, 1982; Schiffries, 1982; Sharpe, 1985; Viljoen and Scoon, 1985; Hart and Kinloch, 1989; Kinloch and Peyerl, 1990; Lee and Butcher, 1990; McCandless and Ruiz, 1991; Schiffries, 1992; Eales et al., 1993; Kruger, 1994; and others). However, no single model can account for all of the features that make the Bushveld Complex unique. For example, high concentrations of Pt, Pd, Ir and Rh imply a mantle derivation for the Rustenburg Layered Suite, but Sr isotopic studies require some crustal involvement to explain $^{87}\text{Sr}/^{86}\text{Sr}$ ratios that become more radiogenic with height in the stratigraphy (Kruger and Marsh, 1982; Eales et al., 1985; Sharpe, 1985; Lee and Butcher, 1990). The Re-Os isotope system is useful for studying the Bushveld

Complex, because Os is one of the six PGE and is present in laurite ($[\text{Ru},\text{Ir},\text{Os}]_2\text{S}_2$), the primary Os-bearing mineral in the Bushveld (Kinloch, 1982; Adair et al., 1992). Because of the large fractionation of Re over Os between crust and mantle, any crustal input into Bushveld magmatism should create phases with significantly higher $^{187}\text{Os}/^{188}\text{Os}$ ratios, due to ^{187}Re decay to ^{187}Os . Neither hydrothermal nor magmatic processes will fractionate Os isotopes, and if minerals with very low Re/Os ratios such as laurite are analyzed, then the $^{187}\text{Os}/^{188}\text{Os}$ ratio of the laurite should reflect the Os source incorporated into the laurite at the time of mineralization.

Hart and Kinloch (1989) measured $^{187}\text{Os}/^{188}\text{Os}$ ratios in single laurite grains from the Merensky Reef in the western lobe. The measured ratios were remarkably consistent and highly radiogenic (0.17–0.18), excepting two erlichmanite grains (OsS_2) with $^{187}\text{Os}/^{188}\text{Os}$ ratios near 0.11, the value expected for mantle derivation at 2.06 Ga (Hart and Kinloch, 1989). McCandless and Ruiz (1991; 1993) obtained bulk rock $^{187}\text{Os}/^{188}\text{Os}$ ratios for the Merensky Reef, UG2, and UG1, indicating that radiogenic Os was a system-wide phenomenon that increased with height, and not restricted to the Merensky Reef. The increase in radiogenic Os with height is similar to the radiogenic Sr trend observed in silicates from the same stratigraphic intervals (Kruger and Marsh, 1982; Sharpe, 1985; Eales et al., 1990; Lee and Butcher, 1990). The radiogenic Os and Sr could be from assimilation of lower crust in the magma chamber that fed the Rustenburg Layered Suite, or from interaction of the Rustenburg Layered Suite with the Pretoria Group sedimentary rocks via assimilation and/or hydrothermal processes. In this study, we report the first initial $^{187}\text{Os}/^{188}\text{Os}$ ratios for chromite separates from early-formed chromitites, and propose a crustal assimilation model whereby high Os concentrations and initial $^{187}\text{Os}/^{188}\text{Os}$ ratios were incorporated into the Rustenburg Layered Suite when it formed 2.06 Ga years ago.

*Author to whom correspondence should be addressed (diamonds@geo.arizona.edu).

†Present address: Rio Tinto Research & Development, 1 Research Avenue, Bundoora, Melbourne, Australia 3083

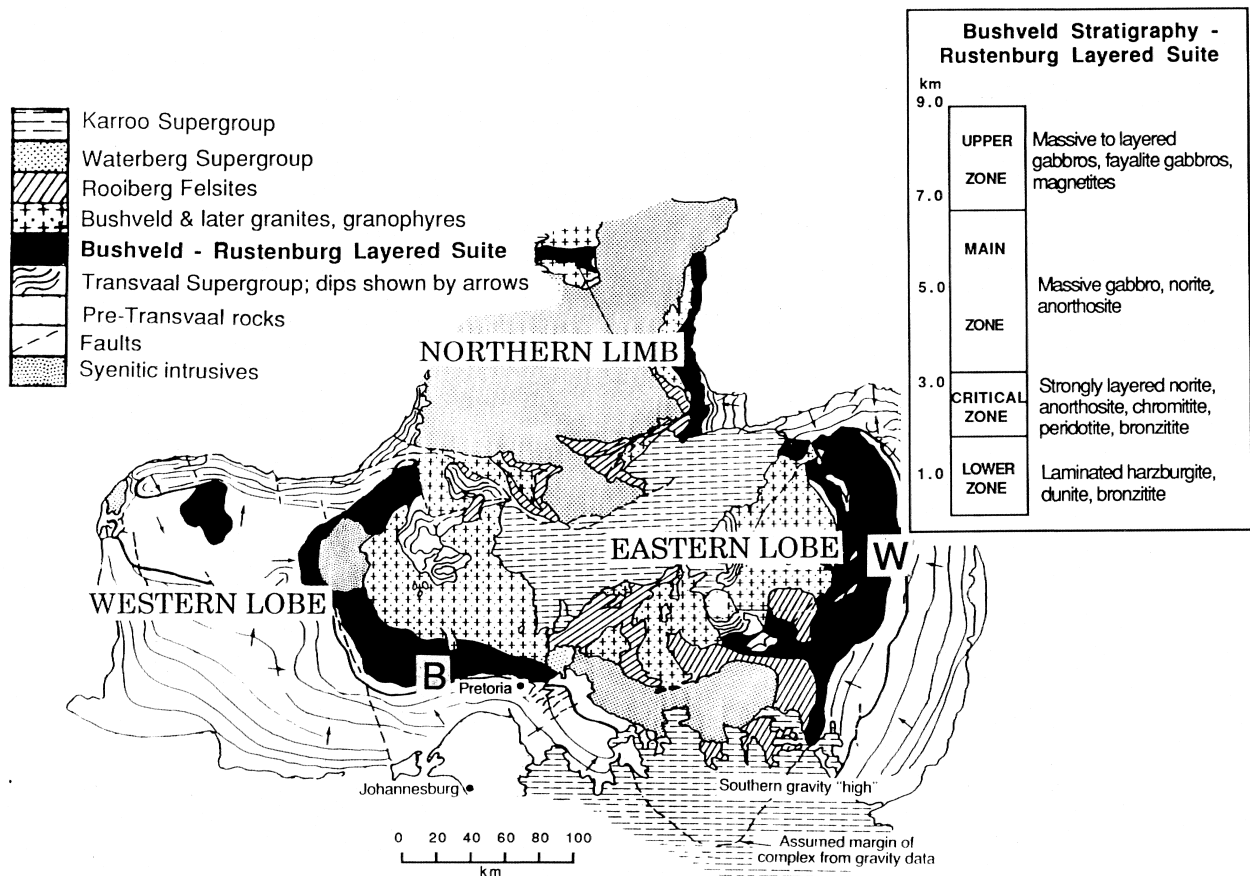


Fig. 1. General geology of the Bushveld Igneous Complex. Rustenburg Layered Suite is black, with locations of Brits (B) and Winterveld (W) as indicated. Transvaal Sequence sedimentary rocks with attitudes relative to horizontal are indicated by the arrows. Post-Transvaal rocks are removed for clarity. (Modified from Guilbert and Park, 1986; Uken and Watkeys, 1997).

2. GEOLOGY OF THE BUSHVELD COMPLEX

The Bushveld Complex *sensu lato* includes two igneous rock assemblages; the ultramafic to mafic Rustenburg Layered Suite (2.061 ± 27 Ga; Walraven et al., 1990), and the Bushveld granites (2.0–1.7 Ga; Walraven et al., 1990; Eriksson et al., 1995). The Rustenburg Layered Suite was emplaced along a regional unconformity between the 2.4–2.5 Ga Pretoria Group rocks and the overlying 2.2 Ga Rooiberg Felsites (Cheney and Twist, 1991; Eriksson et al., 1995; Uken and Watkeys, 1997). The Rustenburg Layered Suite has three areas of relatively continuous outcrop, labeled here as the eastern lobe, western lobe, and northern limb (Fig. 1), which can be further divided into compartments based on structural and lithological variations (Eales et al., 1993; Scoon and Teigler, 1994). These areas, though widely separated, appear to have shared a common magma source, because radiometric ages, chemistry and layering sequences are similar (Sharpe, 1985; von Gruenewaldt et al., 1985; Hatton and von Gruenewaldt, 1987). In spite of the similarities, gravity and magnetic data suggest that the Rustenburg Layered Suite is not continuous beneath cover in the center of the complex, but is comprised of a number of separate intrusions, fed from multiple conduits (Eales et al., 1993). This is borne out in the western lobe, where chemical and mineral-

ogical variations along strike are interpreted to represent a proximal and distal facies relative to a feeder zone located in the northwest (Eales et al., 1993; Scoon and Teigler, 1994; Maier and Teigler, 1995).

The Rustenburg Layered Suite is divided into the Lower, Critical, Main, and Upper zones and varies in thickness from 5 to 9 km (Schiffries and Skinner, 1987; Fig. 1). As many as 25 chromitite layers, some up to 2 m thick, are found in the Critical Zone, and the uppermost of these layers contain economic levels of PGE (Gijbels et al., 1974; Kinloch, 1982; Schiffries and Skinner, 1987). The PGEs are present as sulfides, tellurides, and alloys associated with the upper group or UG1 and UG2 chromitites and the Merensky Reef. Discordant features that disrupt the stratigraphy of the upper Critical Zone include potholes, which modify PGE mineralogy in the layers they cross-cut and require significant volatile activity to account for the changes (Kinloch and Peyerl, 1990). Dunite pipes and iron-rich ultramafic pegmatoids also cross-cut layering and modify PGE mineralogy throughout the lower, critical and main zones (Schiffries, 1982; Peyerl, 1982; Viljoen and Scoon, 1985). Early hydrothermal features include the development of PGE-bearing norite pods along faults and fracture zones (Adair et al., 1994). Mineralogical and field studies also document the presence of

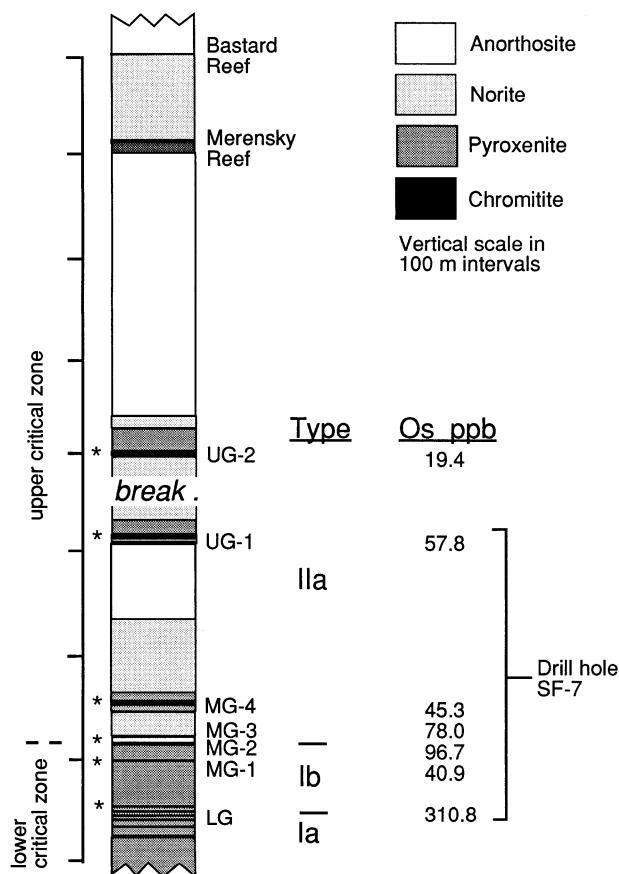


Fig. 2. Upper critical zone stratigraphy of the Brits area, based on drillhole SF-7 (Teigler et al., 1992) and unpublished data. Sampled chromitites are indicated by the asterisk. Osmium concentrations are for Os-bearing phases within chromite grains for each of the indicated layers, as determined in this study.

cross-cutting veinlets filled with hydrothermal minerals and fluid inclusions (Boudreau et al., 1986; Schiffries and Skinner, 1987; Schiffries and Rye, 1989, 1990). It is evident that a variety of magmatic, deuteric and hydrothermal processes have participated in the formation of the Bushveld Complex.

2.1. Chromitites of the Critical Zone

Chromitites of the Rustenburg Layered Suite first appear in the Critical Zone (Fig. 1) and are classified into lower, middle, and upper group chromitites, with individual layers assigned a number (e.g. MG4, UG1). The Lower Group and the MG1 chromitites are associated entirely with ultramafic assemblages, whereas at the base of the MG2 chromitite, noritic-anorthositic cumulates first occur (Fig. 2). This occurrence represents the division between the lower and upper Critical Zone (Scoon and Teigler, 1994). Each chromitite layer appears to be part of a magmatic cycle by association with ultramafic units, although the designation of specific cycles is difficult (Irvine and Sharpe, 1986). Chromitites from the SF-7 core at Brits have been divided into several types based on their position relative to a magmatic cycle (Scoon and Teigler, 1994). Chromitites at the base of cycles associated with harzburgite-pyroxenite or pyroxenite are designated type I (LG1 to MG1), and those that

include anorthosite are type II (Scoon and Teigler, 1994). The Brits compartment is bounded by northwest striking faults with a cumulative vertical displacement of up to 600 meters (Teigler et al., 1992). Faulting appears to be coincident with emplacement of the Rustenburg Layered Suite as hypersthene pyroxenites are developed in the Merensky Reef at fault contacts (McCandless et al., 1994). Table 1 and Fig. 2 indicate where samples were taken from Brits. In the eastern lobe, samples were obtained from exposures in the vicinity of Steelpoort (Merensky Reef, UG2, UG1), and the Winterveld Mine (LG6).

In some samples, veinlets (1–2 mm thick) cross-cut portions of the chromite layers, and increase in abundance in the MG and UG chromitites. Care was taken to avoid sampling in their vicinity as the veinlets cross-cut and displace chromite and intercumulus silicate phases, and contain phlogopite in addition to other hydrous phases.

3. ANALYTICAL METHODS

Chromitites from Brits have a simple mineralogy, consisting of euhedral to subhedral chromite grains 50–1000 microns in diameter, poikilitically enclosed by plagioclase and/or pyroxene crystals up to several cm in diameter. Several polished mounts of 1 mm diameter fragments of the UG2 from Brits were examined by QEM*SEM (Quantitative Evaluation of Materials using Scanning Electron Microscopy) to rapidly assess the occurrence, chemistry and textural associations of PGE phases in the chromitites. QEM*SEM automatically searches through a sample, locates PGE phases, acquires energy dispersive spectra of the PGE phases and all adjoining minerals, and produces a chemical map of each occurrence (McCandless et al., 1994). Most of the Os is in laurite, of which approximately 85% occurs as 10–100 micron diameter inclusions in chromite. Laurite outside the chromite is generally larger (100–200 microns) and is associated with base metal sulfides. Qualitative studies also suggest that most of the Os is also present as laurite inclusions in chromite in the lower and middle group chromitites (Merkle, 1986).

In a previous study, bulk rock measured $^{187}\text{Os}/^{188}\text{Os}$ ratios were obtained by dissolution of PGE phases in boiling 16 N HNO_3 , allowing recovery of Os in a chilled mixture of 10N HCl and ethanol (McCandless and Ruiz, 1991). Chromite and plagioclase remain as a residue in this procedure, and the samples were crushed to a fine powder to ensure complete dissolution of Os-bearing phases included in the chromite. Techniques that ensure complete dissolution of the chromite have been developed (Shirey and Walker, 1995; Freydir et al., 1997). We therefore applied the distillation technique of McCandless and Ruiz (1991) to remove the intergranular Os (i.e., Os-bearing phases outside of the chromite). Unbroken chromites were then separated from the granular residues, and dissolved using the Carius tube technique after Freydir et al. (1997). This approach enabled us to measure Re-Os isotopes for the Os-bearing phases included in the chromite fraction. This approach assumes that laurite is an early crystallizing PGE phase, and that the euhedral to subhedral chromites that comprise the bulk of the chromite layers in the upper Critical Zone are early crystallizing phases from the magma. In this manner, $^{187}\text{Os}/^{188}\text{Os}$ ratios for the earliest formed phases in each layer could be obtained.

A sample of each chromite layer in the SF-7 core was gently crushed so that most chromite grains remained unbroken (Fig. 3a). This was relatively easy as all but the LG chromitites are friable. The crushed product was loaded into a distillation apparatus (after Walker, 1988) with 60 ml of 16 N HNO_3 and 20 ml of H_2O (Mil-Q). The solution was heated to 110°C, and OsO_4 gas was removed from the solution by a nitrogen carrier gas. (McCandless and Ruiz, 1991).

The granular residue from the nitric acid dissolution was rinsed several times in MQ water and dried under a heat lamp. The minerals were sieved to $-1000/+250$ microns and chromite grains were electromagnetically concentrated from plagioclase and plagioclase/chromite intergrowths until >95% chromite grains were obtained. A selection of crystals from each sample were examined by SEM to ensure that they had not been affected by the HNO_3 distillation step. The grains are

Table 1. Summary of Re-Os data for chromitites from the Bushveld.

Location	Sample name	Os	Re	$\frac{^{187}\text{Re}}{^{188}\text{Os}}$	$\frac{^{187}\text{Os}}{^{188}\text{Os}_m}$ in chromite	$\frac{^{187}\text{Os}}{^{188}\text{Os}_i}$	γOs	$\frac{^{187}\text{Os}^*}{^{188}\text{Os}_m}$ intergr.
Western Bushveld								
UG2	16CRM 2 σ	19.42	1.060	0.268	0.164 0.001	0.153	+35.8	0.163 0.006
UG1	112UG1 2 σ	57.85	0.186	0.016	0.141 0.001	0.139	+22.4	0.153 0.004
MG4	111MG4 2 σ	45.32	0.195	0.021	0.1442 0.0002	0.1422	+24.9	0.145 0.005
MG3	110MG3 2 σ	77.98	0.149	0.009	0.145 0.001	0.144	+26.2	0.143 0.005
MG2	109MG2 2 σ	96.68	0.641	0.032	0.133 0.001	0.129	+13.1	0.135 0.005
MG1	108MG1 2 σ	40.92	0.383	0.046	0.1387 0.0004	0.1363	+19.7	0.131 0.004
LG	107LG6 2 σ	310.8	7.440	0.116	0.1442 0.0004	0.1400	+23.0	0.131 0.004
Eastern Bushveld								
UG2	9BV76 2 σ	90.67	0.516	0.028	0.141 0.001	0.14038	+23.3	0.154 0.002
UG1	11BV76 2 σ	61.26	0.965	0.076	0.1410 0.0007	0.13632	+19.7	0.160 0.006
LG6	137LG6 2 σ	92.00	0.100	0.005	0.1293 0.0003	0.1283	+12.7	0.125 0.004
LG5	135LG5 2 σ	—	—	—	—	—	—	0.134 0.006

Re and Os in ppb; uncertainties in concentrations are estimated at 0.1% on average and take into account all steps of the procedure. In chromite 0.924 0 TDos06

virtually unaffected by the nitric acid dissolution (Fig. 3b), thus ensuring that Os-bearing inclusions in the chromite were preserved.

A 100–300 mg split of each chromite separate was loaded into a Carius tube for dissolution and distillation modified from Shirey and Walker (1995) and Freyrier et al., (1997). The sample and a ^{190}Os spike in 10 M HCl is introduced into a chilled Carius tube, allowed to freeze, and followed by 8 ml of 10 M HCl. The ^{185}Re spike in 10 M HCl is added, allowed to freeze, and followed by 8 ml of 15 M HNO_3 . The Carius tube is then sealed with a propane torch and allowed to come to room temperature. The Carius tube is placed in a threaded steel pipe with caps loosely attached and heated to $\sim 240^\circ\text{C}$ for 24h in an oven. The Carius tube is frozen, opened, and the contents of the Carius tube are poured into a distillation apparatus after Walker (1988). The Carius tube is rinsed with 30 ml of 15 M HNO_3 which is added to the distillation flask. A 10 ml volume of 30% H_2O_2 is added drop-wise during heating, which ensures complete oxidation of transition metals including Os (Morgan and Walker, 1989). Boiling temperature is carefully maintained at $\sim 110^\circ\text{C}$ for 2h. After distillation, a 5 ml aliquot is of the pot solution is removed for Pd/Ru measurement, and the remainder is placed in a 100 ml Savillex® PTFE® beaker and evaporated to near dryness. The residue is then brought up in 5 ml of 0.75 N HNO_3 and run through 2 sets of anion columns to recover Re using Bio-Rad® AG-1 X8 200–400 mesh anion resin, with collection in 8 N HNO_3 .

Osmium as $\text{OsO}_4(\text{g})$ passes with a N_2 carrier gas into 6 M NaOH where it undergoes conversion to osmium-hydroxy species. The NaOH trap solution is placed in a clean 50 ml or 125 ml distillation flask, and a clean trap with 4 ml of a 3:1 mixture of 10 M HCl and ethanol is used to trap the Os. Two ml of 10 M H_2SO_4 per ml of NaOH is added to the distillation flask, and distillation takes place at 110°C for 1h. The trap solution is sealed tightly in a threaded 7 ml Savillex® PTFE® vial and heated under a heat lamp to $<80^\circ\text{C}$ for 4 h. Heating of the sealed container is a precaution to ensure that all Os is reduced. The solution is then dried down at $<80^\circ\text{C}$, and 0.4 ml of 0.15 M HCl is added to the vial, which is again sealed tightly and placed under a heat lamp at $<80^\circ\text{C}$ overnight.

Osmium purification was achieved using microcolumns containing a

few beads of Bio-Rad® AG-1 X8 200–400 mesh anion resin. The dried Os sample is brought up in 0.15 HCl and loaded on the resin, and is collected with 0.75 M HCl. The sample is dried down at $<80^\circ\text{C}$ and is ready for loading onto a filament for analysis by negative thermal ionization mass spectrometry (NTIMS, Creaser et al., 1991; Völkening et al., 1991). A Micromass (VG) Sector 54 Mass Spectrometer was used, and total process blanks are 2–7 pg and 4–20 pg for Os and Re, respectively, which is adequate for the present study.

As a matter of course, the OsO_4 gas that was removed during the HNO_3 distillation step was collected in a chilled solution of ethanol and 10 N HCl, diluted 3:1 with Mil-Q water and Os isotope ratios were measured on a Finnigan-MAT SOLA ICP-MS. Mass fractionation was corrected using the $^{188}\text{Os}/^{192}\text{Os}$ ratio and generally amounted to less than 0.5%/amu, with reproducibilities ranging from 2–4% (2s). Only measured $^{187}\text{Os}/^{188}\text{Os}$ ratios could be obtained in this manner, because the intent was to remove this component of Os from the outer surfaces of the chromite grains. The measured $^{187}\text{Os}/^{188}\text{Os}$ ratios are useful for comparative purposes to the chromite separate data, and are to earlier bulk chromitite data obtained in a similar manner (McCandless and Ruiz, 1991). This component of Os, measured from outside the chromite grains, is referred to as the ‘intergranular Os ratio’ in the ensuing discussion.

To obtain Pd/Ru ratios, the 5 ml aliquots collected from the pot solutions of both the nitric and Carius tube distillations were each diluted 4:1 with Mil-Q water. The solutions were scanned on the ICP-MS and the relative intensities of ^{101}Ru and ^{105}Pd were measured. Pd/Ru ratios are in good agreement with bulk chromitite Pd/Ru ratios reported by Scoon and Teigler (1994) for the Brits chromitites.

4. RESULTS

4.1. Os Isotope Stratigraphy in the Bushveld

The intergranular measured $^{187}\text{Os}/^{188}\text{Os}$ ratio (i.e., for Os-bearing phases outside of chromite) is lowest at the LG chromitite (0.131), increasing to 0.163 at the UG2, with a signifi-

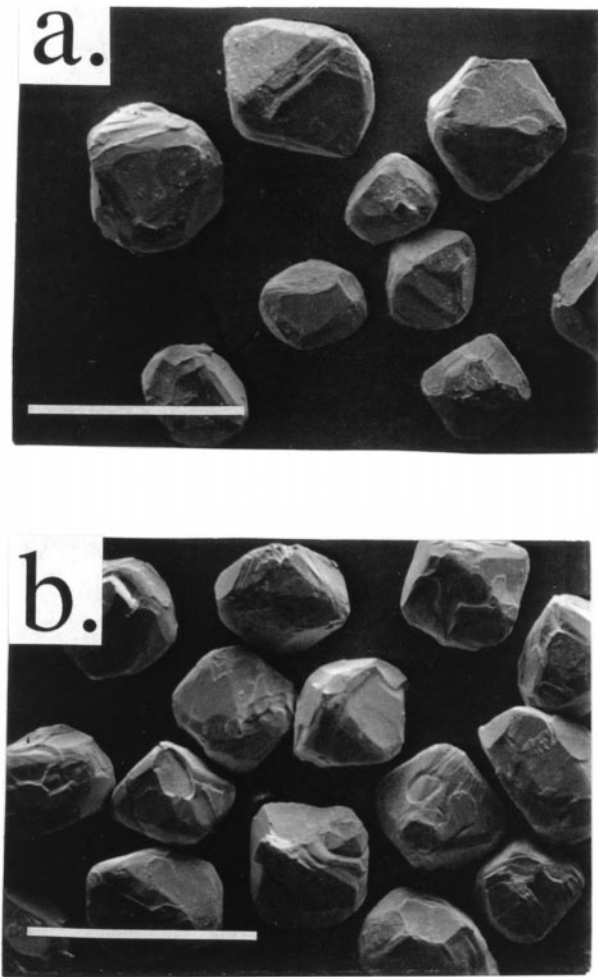


Fig. 3. SEM image of a selection of chromites from the UG1, Brits graben, (a) before and (b) after treatment by nitric acid distillation (see text). The chromites are unaffected by this procedure, ensuring that Os-bearing phases in the chromites are measured in the Carius tube procedure. Scale bar 1000 microns.

cant jump at the lower Critical Zone-upper Critical Zone boundary (Fig. 4a). This trend was observed previously in bulk analyses (McCandless and Ruiz, 1991). For the chromite separates, initial $^{187}\text{Os}/^{188}\text{Os}$ ratios are less radiogenic than the measured intergranular values in the upper Critical Zone, and are more radiogenic than the intergranular values in the lower Critical Zone (Fig. 4a). More radiogenic ratios for intergranular Os in the Upper Zone is expected, as no correction for ^{187}Re decay is made, but the less radiogenic intergranular values in the lower Critical Zone require less radiogenic Os, suggesting that isotopic disequilibrium exists at the hand sample scale. Chromite initial ratios increase with height in the upper Critical Zone, but decrease with height in the lower Critical Zone (Fig. 4a). The inflection at the base of the MG2 coincides with the first occurrence of noritic-anorthositic cumulates (Fig. 2), and is consistent with a new pulse of magma entering the Rustenburg Layered Suite (Scoen and Teigler, 1994). Although less data are available, chromitites from the eastern Bushveld exhibit a similar behavior (Fig. 4b; Table 1).

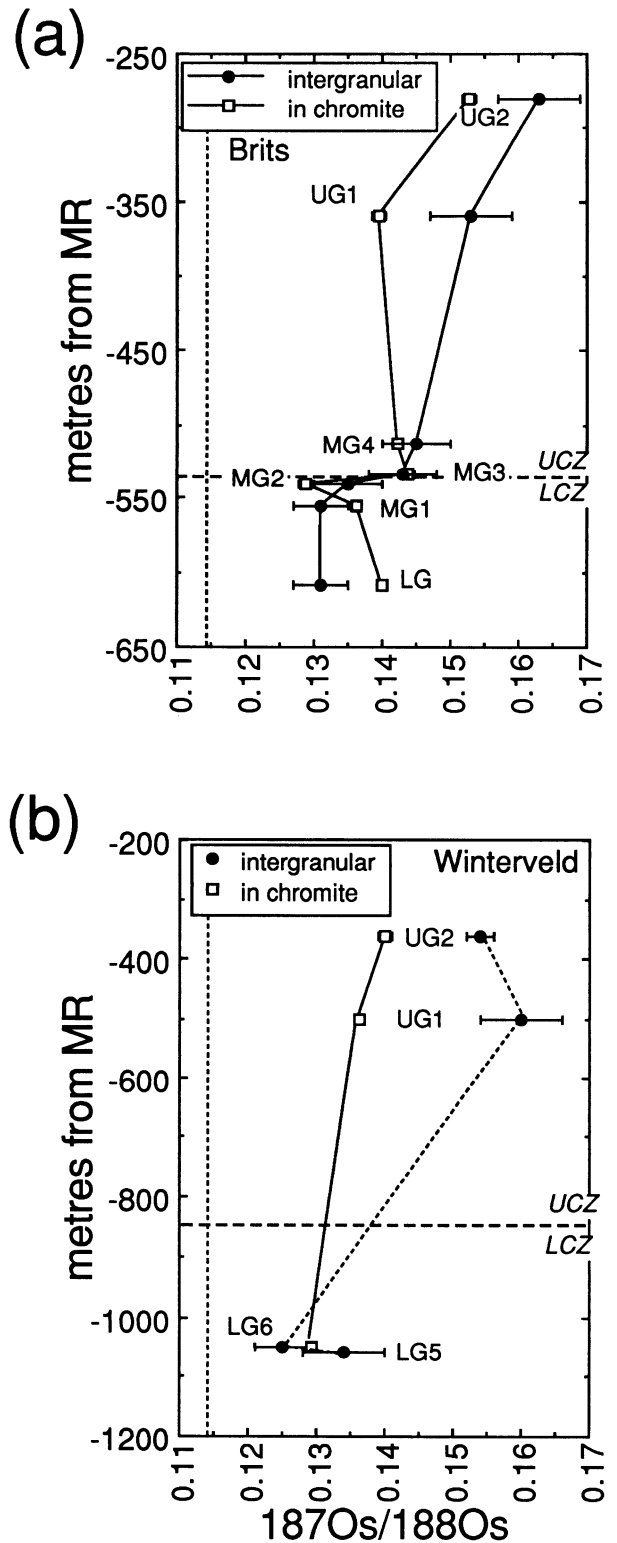
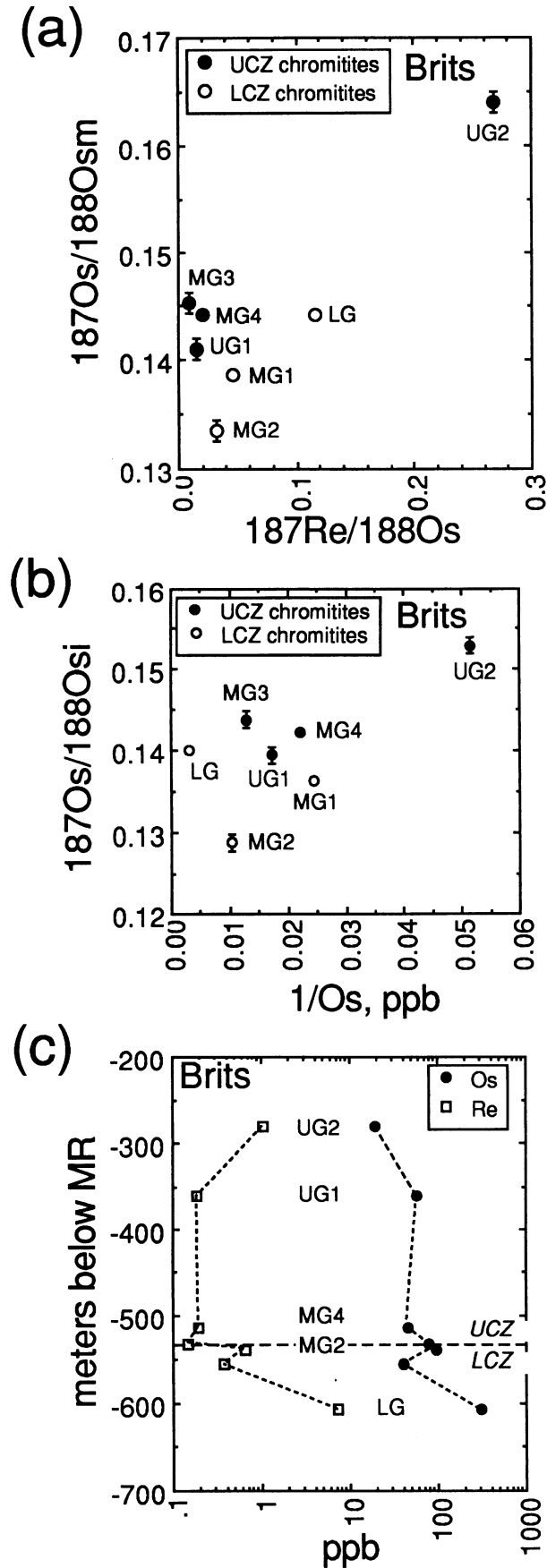


Fig. 4. Measured intergranular $^{187}\text{Os}/^{188}\text{Os}$ (circles), and initial $^{187}\text{Os}/^{188}\text{Os}$ from chromitites (squares) plotted against depth below the Merensky Reef for (a) Brits, western Bushveld and (b) Winterveld, eastern Bushveld. The vertical dashed line at ~ 0.114 is the expected initial value for a magma derived solely from the mantle at ~ 2.06 Ga. Error bars are two sigma. The horizontal dashed line divides the lower and upper Critical Zone, with type I and type II chromites in the lower and upper Critical Zone respectively (after Scoen and Teigler, 1994).



At Brits, there is no obvious correlation between $^{187}\text{Re}/^{188}\text{Os}$ and measured $^{187}\text{Os}/^{188}\text{Os}$ for the Critical Zone chromite separates, therefore only a small component of the radiogenic Os is due to in situ decay of ^{187}Re since the deposit formed (Fig. 5a). None of the chromitites have sufficient Re to correct the measured $^{187}\text{Os}/^{188}\text{Os}$ ratios back to a value of ~ 0.11 expected for a mantle-derived magma at 2.06 Ga.

There is also no strong positive correlation between initial $^{187}\text{Os}/^{188}\text{Os}$ ratios and $1/\text{Os}$ observed for the upper Critical Zone chromitites, indicating that no simple, single stage mixing model is apparent for the addition of radiogenic Os (Fig. 5b). Chromitites in the lower Critical Zone also exhibit no pattern, with the LG chromite having the highest Os content of any chromitites analyzed (310.8 ppb), and maintaining a radiogenic initial ratio (0.140). For the Critical Zone, a simple mixing model is unlikely to account for these earliest radiogenic initial $^{187}\text{Os}/^{188}\text{Os}$ ratios recorded in the chromitites.

A further distinction between the lower Critical Zone and upper Critical Zone chromite separates is also revealed by comparing the absolute abundances of Re and Os. Both Re and Os vary by orders of magnitude in the lower Critical Zone chromitites, but exhibit the same relative shifts in abundance from one layer to the next (Fig. 5c). In the upper Critical Zone, Re and Os exhibit opposite shifts i.e., an increase in Re correlates with a decrease in Os (Fig. 5c). This behavior may relate to a change in crystallization of silicate, oxide, and PGE phases at the base of the upper Critical Zone, possibly due to an influx of new magma as suggested by earlier studies (Teigler et al., 1992).

5. DISCUSSION

5.1. Mantle/Core Source Heterogeneities

The low Re/Os ratios, coupled with radiogenic initial $^{187}\text{Os}/^{188}\text{Os}$ ratios for the chromite separates raises the possibility that mantle source heterogeneities are the cause. Walker et al., (1994) suggest that Os isotopic variations in sulfide ores from the Noril'sk PGE deposit in Siberia are largely a reflection of mixing between heterogeneous mantle sources. Values of γ_{Os} up to +12 are higher than predicted for the mantle at the time of formation for the Noril'sk sulfide ores (Walker et al., 1994), and a similar scenario has been suggested for ferropicrites from the Pechenga Complex (Walker et al., 1997a). Picrites and tholeiites from the Keweenaw rift also have been ascribed to an enriched mantle source, with maximum γ_{Os} values of +12 (Shirey, 1997). In comparison, g_{Os} for the Rustenburg Layered Suite chromitites ranges from +12 to +35 (Table 1). Crustal contamination rather than mantle heterogeneity must account for the more radiogenic γ_{Os} values in the Bushveld. For comparison, similar and higher values recently observed for continental rift basalts in Death Valley have been ascribed to crustal contamination (+36 to +1730; Asmerom and Walker, 1998). If the Bushveld magmas were derived from a heterogeneous mantle source with OIB-type Os characteristics, variations like those observed at Noril'sk or in the Keweenaw would be

Fig. 5. (a) $^{187}\text{Re}/^{188}\text{Os}$ versus measured $^{187}\text{Os}/^{188}\text{Os}$, (b) initial $^{187}\text{Os}/^{188}\text{Os}$ versus $1/\text{Os}$, and (c) Os and Re concentration versus depth below Merensky Reef for chromitites from Brits.

masked by the much more radiogenic contributions arising from crustal contamination.

Recent developments in the ^{190}Pt - ^{186}Os isotope system suggest that enrichments in $^{186}\text{Os}/^{188}\text{Os}$ in mafic magmas could be due to contributions of radiogenic Os from the core-mantle boundary, and that coupled enrichments in $^{186}\text{Os}/^{188}\text{Os}$ and $^{187}\text{Os}/^{188}\text{Os}$ might distinguish core-mantle from mantle-crust reservoirs (Walker et al., 1995, 1997a; Brandon et al., 1998). The core is assumed to be enriched in both Re and Pt over the mantle, such that small amounts of outer core material mixed into the lower mantle would produce a distinctive core isotopic signature (Shannon and Agee, 1998). A contribution from the core to the Rustenburg Layered Suite cannot be entirely excluded, but is beyond the scope of the present study.

5.2. Crustal Assimilation Models

Parental magmas for the Rustenburg Layered Suite are believed to be represented by mafic-ultramafic sills adjacent to and beneath the Lower Zone that have tholeiitic, boninitic, and peridotitic compositions (Davies and Tredoux, 1985; Harmer and Sharpe, 1985; Sharpe and Hulbert, 1985). Merkle et al., (1995) analyzed PGE from a selection of the sills and report Os below detection limits (<3 ppb) in all cases. The total thickness of chromitites from drillhole SF-7 is roughly 13.5 meters (from Teigler et al., 1992; Fig. 2), with a weighted average of 0.13 ppb Os present over that accumulation. The Rustenburg Layered Suite in the Brits compartment is roughly 5000 meters thick, and assuming an average density of 4.5 g cm^{-3} for chromite and 3.0 g cm^{-3} for the section as a whole, an average of 0.27 ppb Os is obtained for the Brits section. This is a minimum estimate because it does not account for Os in the lower LG chromites, nor in the Merensky Reef. We use a tholeiitic composition transitional to komatiite (0.14 ppb Os; K-tholeiite) and a true komatiite (1.38 ppb Os; after Walker et al., 1991) as possible parental magmas, because Os contents are between the calculated minimum and the 3 ppb Os detection level reported by Merkle et al. (1995).

Contact metamorphic facies indicate that the Rustenburg Layered Suite was emplaced into Pretoria Group rocks at 10–15 km depth and 700–800°C (Sharpe and Hulbert, 1985; Uken and Watkeys, 1997). These conditions require that the magma chamber feeding the Rustenburg Layered Suite must have resided in the lower crust. Granulitic lower crust beneath the Transvaal Basin is evidenced by granulite xenoliths in the Schuller and Premier kimberlites which are emplaced through the southern edge of the Bushveld Complex (D. de Bruin, pers. comm., 1995). Using a mafic granulite composition (1.21 ppb Re, 0.10 ppb Os; Saal et al., 1998), and assuming that it was extracted from the mantle at ~ 3 Ga, about 5% addition to a K-tholeiite parent magma will account for $^{187}\text{Os}/^{188}\text{Os}$ initial ratios up to 0.153 (Fig. 6a). A felsic granulite is a less adequate contaminant, requiring up to 25% assimilation, which would significantly alter the bulk composition of the resultant magma. In comparison, no amount of mafic or felsic granulite can be added to a komatiitic parent magma to obtain the observed initial values (Fig. 6b).

The thermal aureole produced by emplacement of Rustenburg Layered Suite extends over 20 kilometers into Pretoria Group country rocks (Sharpe and Hulbert, 1985; Uken and

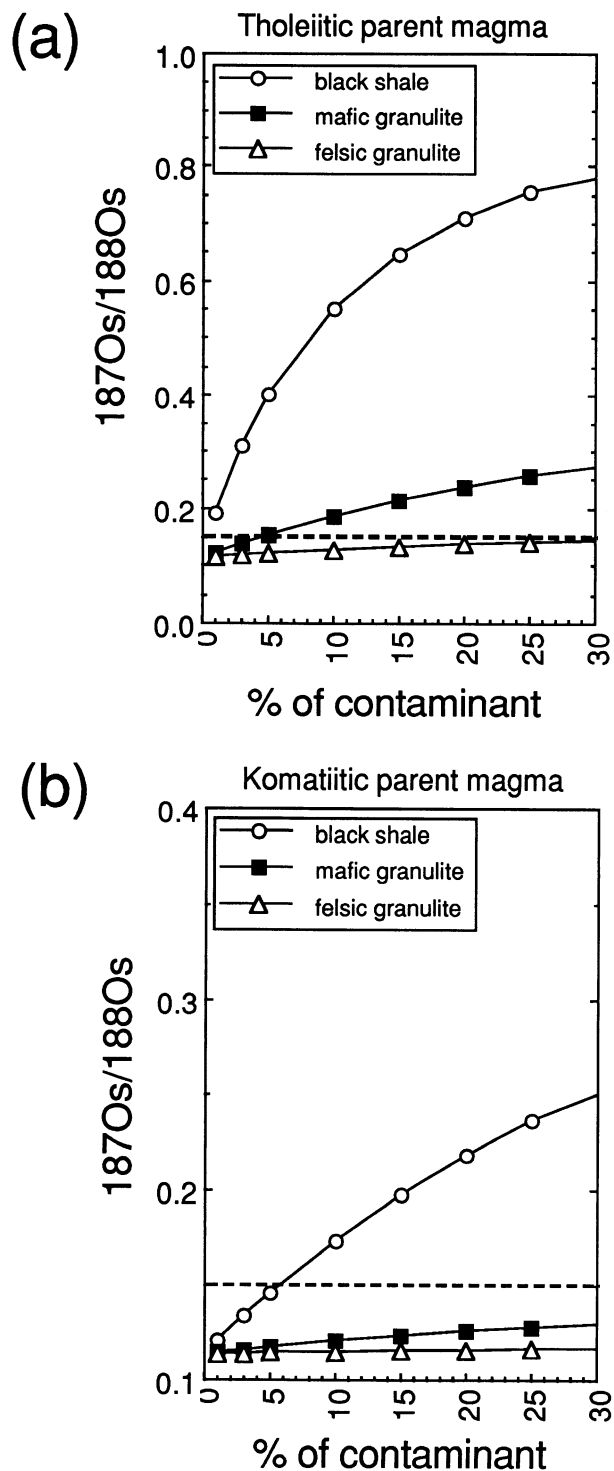


Fig. 6. Effects of crustal assimilation on (a) K-tholeiite and (b) komatiitic parent magmas, using black shale, felsic granulite, and mafic granulites as contaminants. Horizontal dashed line indicates the $^{187}\text{Os}/^{188}\text{Os}$ initial ratio of 0.153 for the UG2. Parent magma concentrations are 2.33 ppb Re, 0.14 ppb Os for K-tholeiite; 0.54 ppb Re, 1.37 ppb Os for komatiite (from Walker et al., 1991). Granulite compositions (mafic 0.121 ppb Re, 0.10 ppb Os; felsic 0.22 ppb Re, 0.06 ppb Os) from Saal et al., 1997. Black shale composition (1.49 ppb Os, 1.3 ppb Re) from Revizza and Turekian, 1989.

Watkeys, 1997). Nearly 60% of the country rock in contact with the Bushveld complex is shale, including pyritic black shale (Button, 1976; Cheney and Twist, 1991; Eriksson et al., 1995). Black shale can have high Re and Os concentrations, acquiring large concentrations of radiogenic Os over time (Ravizza and Turekian, 1989). Assuming a shale with Re and Os concentrations of 1.3 and 1.5 ppb respectively (Ravizza and Turekian, 1989) and an age of 2.3 Ga, much less than 1% in a tholeiitic parent magma will produce $^{187}\text{Os}/^{188}\text{Os}$ ratios of 0.15 (Fig. 6a). Assimilation of 5% black shale into a komatiitic parent magma can produce similar results (Fig. 6b). Assimilation of black shale may thus explain some of the small-scale Os isotopic heterogeneities observed in the individual chromitite layers (Fig. 4), but it is difficult to envision that this mixing would be efficient enough to produce the nearly identical initial $^{187}\text{Os}/^{188}\text{Os}$ ratios observed over the entire Bushveld.

It is important to note that both komatiitic and tholeiitic magmas have higher $^{187}\text{Re}/^{188}\text{Os}$ ratios than those recorded in the Rustenburg Layered Suite chromitites. Either parent magma would therefore evolve from a mantle value of 0.11 at 2.06 Ga, to a present-day $^{187}\text{Os}/^{188}\text{Os}$ greater than what is measured in the Rustenburg Layered Suite chromitites. The absence of Re is to be expected, since laurite has an apparent affinity for chromite and is a natural sink for Os (Merkle, 1986; McCandless et al., 1994). It is possible that the Re initially present in either the K-tholeiite or komatiite parent magma, precipitated into base metal sulfide phases elsewhere in the Rustenburg Layered Suite. This is supported by preliminary data for sulfide-rich zones in the Main and Upper Zone, that indicate concentrations of 2–5 ppb Re and <100 ppt Os (McCandless, unpublished data).

5.3. Platinum Group Element Mineralization

There are several styles of PGE mineralization in the Bushveld Complex (von Gruenewaldt et al., 1990), but the most significant with respect to production and reserves is the PGE mineralization associated with chromitites. Numerous detailed theories have been proposed to account for PGE mineralization in the Bushveld that are beyond the scope of this study, but can be generalized into two dominant theories. One theory is that PGE precipitation occurs solely through magmatic processes, which may involve either differentiation of a single magma pulse, or mixing with a new magma pulse to trigger mineralization (Liebenberg, 1969; Sharpe et al., 1981; Hatton, 1986; Irvine and Sharpe, 1986; Naldrett and von Gruenewaldt, 1988; Eales et al., 1990; Naldrett et al., 1990; Teigler and Eales, 1993; Scoon and Teigler, 1994). The second theory requires fluids to concentrate PGE into economic horizons. Some believe that late magmatic-early deuteritic fluids remelt early-formed phases, scavenging PGE from them, then recrystallizing (Boudreau et al., 1986; Mathez et al., 1992; Nicholson and Mathez, 1991). Others propose that hydrothermal fluids migrate upward through the nearly solidified layers, scavenging PGE from partially crystallized chromitites, with most PGE ending up in the Merensky Reef. Where the fluids reach critical concentrations, they completely alter layering to produce fluid-enriched pothole and pipe structures (Schiffries, 1982; Ballhaus and Stumpfl, 1986; Stumpfl, 1986; Ballhaus et al., 1988; Ballhaus and Ryan, 1995).

Although there is some uncertainty in the relative incompatibilities of the six PGE in magmatic processes, it is generally accepted that Pd is more incompatible than Ru, Ir, and Os (Barnes et al., 1985). It is also believed that Ru and Os are less soluble than Pd in acidic solutions (Mountain and Wood, 1988). Most of the Os and Ru in the upper Critical Zone chromitites is in laurite inclusions in chromite, whereas Pd is found in intergranular PGE in association with base metal sulfides (Merkle, 1986; Adair et al., 1994). The mineralogical influence of laurite on the Pd/Ru ratio is strongly evident, with order of magnitude differences in the chromite separates versus intergranular fractions (Fig. 7). Tie-lines that connect the chromite and intergranular fractions for each chromitite layer cross over each other, exhibiting no systematic behavior that might be expected if all the PGE were precipitated solely by magmatic processes (Fig. 7a). Differences in the Pd/Ru ratio for each chromitite layer are reflected in the length of each tie-line, representing a 2 orders of magnitude difference for the lower Critical Zone chromitites, to a 4 orders of magnitude difference for the upper Critical Zone chromitites (Fig. 7a). These trends suggest that the mobile PGE (represented by Pd) become enriched in the upper Critical Zone, similar to observations by Scoon and Teigler (1994).

If a fluid-dominant (deuteritic/hydrothermal) process caused upward enrichment of PGE, it may be expected that the laurite (and any other PGE minerals) included in chromite would be shielded from this process. Under these conditions, the Pd/Ru ratios for the chromite separates should be different from the intergranular fraction of the same sample. Instead, the relative shift in the Pd/Ru ratio for the intergranular and chromite fractions is similar from one layer to the next i.e., the intergranular Pd/Ru ratio decreases from the LG to the MG1, increases slightly to the MG2, then significantly from the MG2 to the MG3 (Fig. 7b). The Pd/Ru ratio for the chromite fraction is at least an order of magnitude greater, but its Pd/Ru ratio nevertheless exhibits the same shift from one layer to the next (Fig. 7b). The pattern suggests that the source of PGE in the chromite grains is the same as that which precipitated PGE as intergranular phases. This relationship suggests that the intergranular PGE were precipitated shortly after the chromite crystallized, as part of the same processes that formed each individual chromitite layer, and were unaffected by later deuteritic or hydrothermal fluids. Although some local Os isotopic disequilibrium exists within individual chromitites (Fig. 4, 7a), the results do not support post-layering mobilization of PGE into a specific chromite layer (e.g. UG2) from other chromitite layers in the system.

The UG2 at Brits is the most enriched of the chromitites with respect to total PGE (Scoon and Teigler, 1994) and it also has the highest initial $^{187}\text{Os}/^{188}\text{Os}$ ratio of any chromitite at Brits (0.153). Although less data are available, similar results exist for the Winterveld chromitites (Fig. 4b). This suggests that some positive correspondence exists between crustal assimilation and PGE accumulation. It is possible that a more contaminated magma has increased levels of volatiles, sulfur or some other component that is necessary for PGE precipitation to occur. A similar process is proposed for base metal mineralization in subduction zones, where H_2O , sulfur or metals are enhanced in magmas that interacted with lower crust (McCandless and Ruiz, 1993).

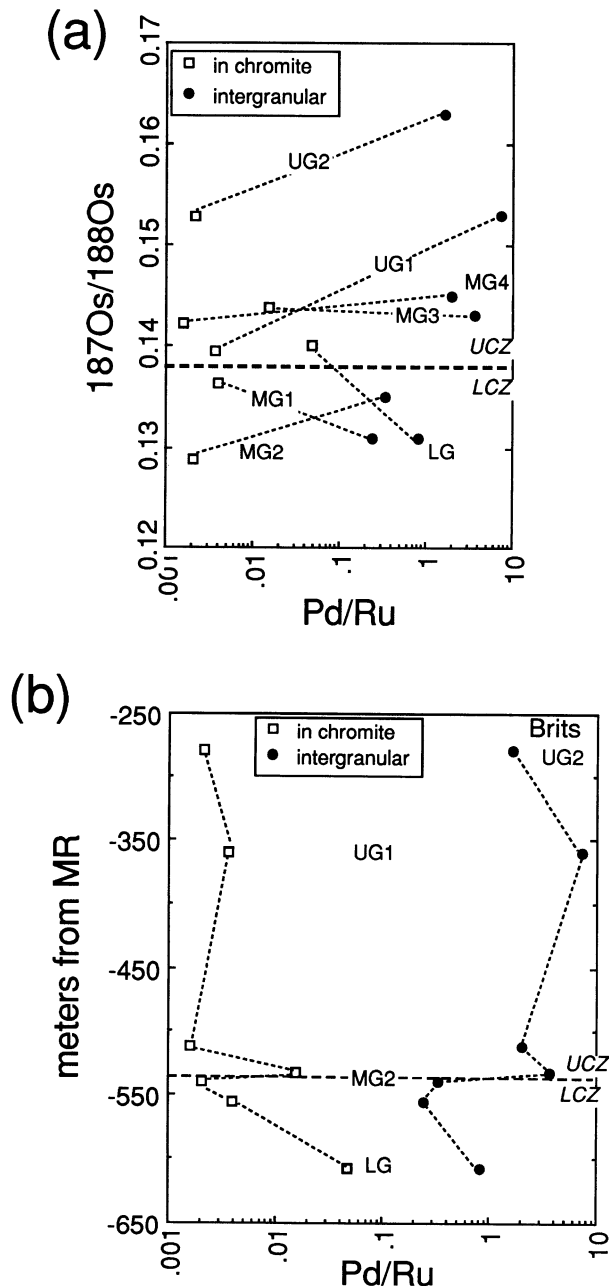


Fig. 7. (a) Pd/Ru ratios versus $^{187}\text{Os}/^{188}\text{Os}$ ratios, (b) Pd/Ru ratios versus depth below Merensky Reef for intergranular (circles) and chromitite (squares) fractions.

Although the $^{187}\text{Re}/^{188}\text{Os}$ ratio is also very high for the UG2 (0.164; Table 1), the chromitite corrects to an initial $^{187}\text{Os}/^{188}\text{Os}$ ratio similar to bulk initial $^{187}\text{Os}/^{188}\text{Os}$ values from elsewhere in the western lobe (e.g., 0.154–0.156 at Rustenburg; McCandless unpublished data). Thus elevated $^{187}\text{Re}/^{188}\text{Os}$ ratios are not indicative of high PGE content in the UG2 chromitite.

6. EMPLACEMENT MODEL FOR THE RUSTENBURG LAYERED SUITE

The following model is based on Os, Sr and geophysical studies of the Bushveld Complex. Geophysical data indicate

that the Archean basement is thinner beneath the Transvaal Basin compared to elsewhere in the region, which may have been due to uplift and erosion. Loading on this thinner basement led to the formation of the Transvaal Basin, with a concomitant melting of the crust and mantle beneath the basin (Kruger and Corner, 1987). The clastic and volcanic rocks of the Pretoria Group were deposited in the Transvaal Basin prior to emplacement of the Rustenburg Layered Suite, and reflect derivation from granitic to basaltic sources associated with an intracontinental rift environment (Schreiber et al., 1992).

The critical point of deposition in the Transvaal Basin was the eruption of the Rooiberg Felsites, represented by 200,000–300,000 km³ of lavas that are up to 5 km in thickness (Eriksson et al., 1995). The Rooiberg Felsites are a critical feature, because their voluminous outpouring indicates that significant heating of basement rocks (and presumably mantle) has taken place beneath the Transvaal Basin. Shortly after eruption of the Rooiberg Felsites, the parental magma to the Rustenburg Layered Suite ponded near the crust-mantle boundary (Fig. 8). This parental magma assimilates 3%–5% mafic granulitic lower crust, with assimilation being greatest on margins of the magma chamber and less in the center. Concomitant with assimilation of granulitic crust, some phases crystallize in the chamber, increasing the average density of the magma along the contact (Fig. 8). Hotter and less dense magma from the center of the chamber is the first to ascend into the Transvaal Basin, mixing in a component of crustally contaminated magma during its ascent (time t_1 ; Fig. 8). This first pulse is a mixture of denser, contaminated, partially crystalline magma, and less dense primitive magma. The denser material settles to form the lower zone, and the less contaminated, less dense magma becomes the lower Critical Zone. Decreasing initial $^{187}\text{Os}/^{188}\text{Os}$ ratios from the LG to the MG2 chromitite record the culmination of this first pulse in the lower Critical Zone. The magma source at the mantle-crust boundary continues to assimilate lower crust, and as successive pulses of magma ascend, they introduce greater amounts of radiogenic Os into the Transvaal Basin (times t_2 , t_3 , Fig. 8).

Figure 8 depicts the emplacement of the Rustenburg Layered Suite in three major pulses, but emplacement of the Rustenburg Layered Suite magmas into the Transvaal Basin must have been nearly instantaneous, without a significant hiatus between major pulses. A rapid emplacement rate is required because the lobes of the Rustenburg Layered Suite are actually thin sills, when properly scaled (horizontal bars, Fig. 8). Assuming a magma with initial temperature of 1300°C and wall rocks at a temperature of 250°C (Cawthorn and Walraven, 1997; Uken and Watkeys, 1997), a 1.5 km thick magma pulse (representing the Lower Zone, for example) could not be slowly emplaced over lateral distances of 150 km without completely crystallizing first. Thermal modeling thus requires an emplacement rate for the Rustenburg Layered Suite of greater than 6 km³ yr⁻¹ (Cawthorn and Walraven, 1997), which is nearly 2 orders of magnitude greater than eruption rates estimated for some flood basalts (0.09 km³ yr⁻¹, Hooper, 1988). Thus, much of the system-wide chemical, mineralogical, and isotopic evolution observed in the Rustenburg Layered Suite must have taken place in the magma chamber that resided near the crust-mantle boundary.

Evidence for differentiation and crystallization in the paren-

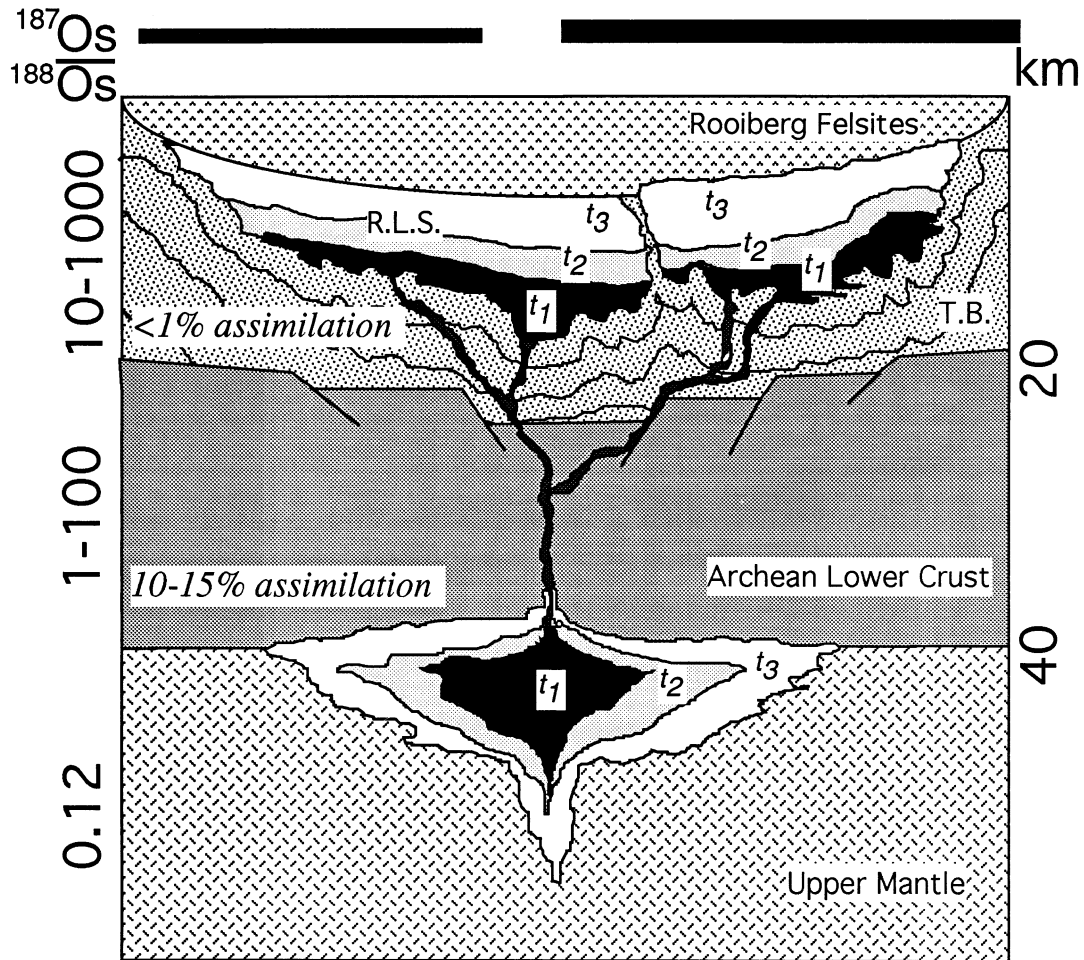


Fig. 8. Schematic representation of the emplacement of the Rustenburg Layered Suite. Depths for emplacement of the Rustenburg Layered Suite, and for the crust-mantle boundary are given in kilometers, and $^{187}\text{Os}/^{188}\text{Os}$ ratios for rock types are estimated along the left margin. The horizontal dimension is greatly compressed in this figure. For comparison, the true thickness:length relations are represented by the horizontal bars above the figure, using 9 km thickness for the eastern lobe and 7 km thickness for the western lobe. Following sagging, extension, and heating of the Archean basement, a pulse of magma ponds near the lower crust-upper mantle boundary. Assimilation of 1–5% lower crust takes place, being greatest along the margins of the magma chamber, and less prevalent in the center. Magma from the center of the chamber begins its ascent into the Transvaal Basin at time t_1 , forming the lower zone (black). Intermediate regions of the magma chamber are depleted at time t_2 to form the critical zone (dark gray), with an increasingly greater crustal component in this magma. Magma from near the margins of the chamber erupt into the Transvaal Basin at time t_3 , forming the main and upper zones (light gray). Emplacement of the Rustenburg Layered Suite is conformable along the contact between the upper Pretoria Group and the Rooiberg Felsites, and diapiric deformation of the Pretoria Group ensues. Less than 1% of Pretoria Group shales are assimilated into the RLS at the time of emplacement.

tal magmas that fed Rustenburg Layered Suite includes the presence of phenocrysts in the early, chilled marginal rocks, compositional disequilibrium in orthopyroxene and plagioclase crystals in single layers, and Sr isotopic disequilibrium in plagioclase grains from some upper Critical Zone horizons (Eales et al., 1993; Kruger, 1994; Rice and Eales, 1995; McCandless, unpub. data). Regional similarities in $^{187}\text{Os}/^{188}\text{Os}$ along strike for the Merensky Reef (Hart and Kinloch, 1989), and for the chromitite layers that are widely separated (McCandless and Ruiz, 1991; Fig. 4) also suggest that most of the Os must have been incorporated into the magmas before they reached the Transvaal Basin.

In the Transvaal Basin, emplacement of the Rustenburg Layered Suite is roughly along the contact between the upper

Pretoria Group and the Rooiberg Felsites (Cheney and Twist, 1991). The Rustenburg Layered Suite magma had an initial density of 2.58 g/cm^3 at the time of initial emplacement, which increased with the presence of crystallizing phases in the magma (Rice and Eales, 1995). Shales range in density from $2.1\text{--}2.7 \text{ g/cm}^3$ (Turcotte and Shubert, 1982), and diapirism and deformation of the shales ensued because the Rustenburg Layered Suite magmas found it easier to flow outward and downward into the nearly isopycnal shales than to rise through the massive Rooiberg Felsites (Vermaak, 1970; Uken and Watkeys, 1997; Fig. 8). Preserved contacts of the Rustenburg Layered Suite with Pretoria Group rocks are rare, but suggest that assimilation of shales was not widespread (Cheney and Twist, 1991; Uken and Watkeys, 1997). Where assimilation of

shales did occur, alkalis, Fe, and Mg were taken into the magma, leaving aluminous to granitic rocks at the contacts (Willemse and Viljoen, 1970). These observations are consistent with the Os data that predict that less than 1% of black shales could have been assimilated into the Rustenburg Layered Suite (Fig. 6).

7. CONCLUSIONS

Rhenium-osmium isotopes from chromitites in the Rustenburg Layered Suite have provided new constraints on the formation of the Rustenburg Layered Suite of the Bushveld Complex. Measured $^{187}\text{Os}/^{188}\text{Os}$ ratios on intergranular phases show an increase to more radiogenic values with height in the igneous stratigraphy. Initial $^{187}\text{Os}/^{188}\text{Os}$ ratios for chromite separates are also radiogenic even at the lowest chromitite layer, indicating that radiogenic Os must have been present in the magma source that fed the Rustenburg Layered Suite into the Transvaal Basin. Granulitic lower crust is present beneath the Transvaal Basin, and roughly 5% assimilation of mafic granulite into a tholeiitic parent magma can account for the radiogenic $^{187}\text{Os}/^{188}\text{Os}$ ratios.

Lower crustal assimilation best explains the similar $^{187}\text{Os}/^{188}\text{Os}$ ratios that are observed for individual chromitite layers across the complex. Variable assimilation of <1% of Pretoria Group shales, due to lithologic and thermal variations along the contact, may explain some erratic $^{187}\text{Os}/^{188}\text{Os}$ ratios observed for chromite separate and intergranular fractions within a single chromitite. The introduction of radiogenic Os by hydrothermal fluids would also lead to heterogeneity at this scale. The relatively consistent initial $^{187}\text{Os}/^{188}\text{Os}$ ratios for chromitite separates from across the complex suggests that most of the radiogenic Os was incorporated into the magma before it was emplaced into the Transvaal Basin.

Internally consistent Os isotope and Ru/Pd ratios for each chromitite layer suggest that the most of the PGE were concentrated into chromitite layers shortly after crystallization of the chromite. Higher Pd/Ru ratios in the UG2 are probably not due to post-solidus mobilization of intergranular PGE in residual fluid or magma (Stumpfl, 1986), which agrees with chemical trends for silicate layers in the upper Critical Zone (Cawthorn; 1996).

Acknowledgments—This study was made possible with the consent and cooperation of various South African mining houses, including Golden Dumps (Crocodile River Mine), Rand Mines, and Genmin. Funding was provided by NSF grants EAR9406259, EAR9628150, EAR9708361 and by the W.M. Keck Foundation, which funded some of the analytical equipment. Access and use of the QEM*SEM was made possible through the CSIRO, Brisbane, Australia. Meticulous chromite sample preparations and mineral separations were accomplished by S.M. Torba. Comments from Yemane Asmerom and two anonymous reviewers led to improvement of the manuscript.

REFERENCES

- Adair B. I., Wilke G., Ruiz J., and McCandless T. E. (1994) Osmium isotopic disequilibrium in the Bushveld Complex. *Eos* **75**, 710.
- Asmerom Y. and Walker R. J. (1998) Pb and Os constraints on the composition and rheology of the lower crust. *Geology* **26**, 359–362.
- Ballhaus C. and Ryan, C. G. (1995) Platinum-group elements in the Merensky Reef I: PGE in solution in base metal sulfides and the down-temperature equilibrium history of Merensky Ores. *Cont. Min. Pet.* **122**, 241–251.
- Ballhaus C. G. and Stumpfl E. F. (1986) Sulfide and platinum mineralization in the Merensky Reef: Evidence from hydrous silicates and fluid inclusions. *Cont. Min. Pet.* **94**, 192–204.
- Ballhaus C. G., Cornelius M., and Stumpfl E. F. (1988) The upper Critical Zone of the Bushveld Complex and the origin of Merensky-type ores—A discussion. *Econ. Geol.* **83**, 1082–1085.
- Barnes S.-J., Naldrett A. J., and Gorton M. P. (1985) The origin of the fractionation of platinum-group elements in terrestrial magmas. *Chem. Geol.* **53**, 303–323.
- Boudreau A. E., Mathez E. A., and McCallum, I. S. (1986) Halogen geochemistry of the Stillwater and Bushveld Complexes: Evidence for transport of the platinum-group elements by Cl-rich fluids. *J. Pet.* **27**, 967–986.
- Brandon A. D., Walker R. J., Morgan J. W., Norman M. D., and Prichard, H. M. (1998) Coupled ^{186}Os and ^{187}Os evidence for core-mantle interaction. *Science* **280**, 1570–1573.
- Button A. (1976) Stratigraphy and relations of the Bushveld floor in the eastern Transvaal. *Geol. Soc. South Africa Trans.* **79**, 3–12.
- Cawthorn R. G. and Walraven F. (1997) The Bushveld Complex: A time to fill and a time to cool. *Econ. Geol. Res. Unit Inf. Circ.* **307**, Univ. Witwatersrand, 11 p.
- Cheney E. S. and Twist D. (1991) The conformable emplacement of the Bushveld mafic rocks along a regional unconformity in the Transvaal succession of South Africa. *Precambrian Res.* **52**, 115–132.
- Creaser R. A., Papanastassiou D. A., and Wasserburg G. J. (1991) Negative thermal ion mass spectrometry of osmium, rhenium, and iridium. *Geochim. Cosmochim. Acta* **55**, 397–401.
- Davies G. and Tredoux M. (1985) The platinum-group element and gold contents of the marginal rocks and sills of the Bushveld Complex. *Econ. Geol.* **80**, 838–848.
- Eales H. V., Botha W. J., Hattingh P. J., de Klerk W. J., Maier W. D., and Odgers A. T. R. (1993) The mafic rocks of the Bushveld Complex: a review of emplacement and crystallization history, and mineralization, in the light of recent data. *J. African Earth Sci.* **16**, 121–142.
- Eriksson P. G., Hattingh P. J., and Altermann W., (1995) An overview of the Transvaal Sequence, Bushveld Complex, South Africa. *Mineral. Dep.* **30**, 98–111.
- Freydier C., Ruiz J., Chesley J. T., McCandless T. E., and Munizaga F. (1997) Re-Os systematics of sulfides from felsic igneous rocks: Application to base metal porphyry mineralization in Chile. *Geology* **25**, 775–778.
- Gijbels R. H., Millard H. T. Jr., Desborough G. A., and Bartel A. J. (1974) Osmium, ruthenium, iridium, and uranium in silicates and chromite from the eastern Bushveld Complex, South Africa. *Geochim. Cosmochim. Acta* **38**, 319–337.
- Guilbert J. M. and Park C. F. Jr. (1986) *The Geology of Ore Deposits*. New York, W. H. Freeman and Co., 985 p.
- Harmer R. E. and Sharpe M. R. (1985) Field relations and strontium isotope systematics of the marginal rocks of the eastern Bushveld Complex. *Econ. Geol.* **80**, 813–837.
- Hart S. R. and Kinloch E. D. (1989) Osmium isotope systematics in Witwatersrand and Bushveld ore deposits. *Econ. Geol.* **84**, 1651–1655.
- Hatton C. J. (1986) Densities and liquidus temperatures of Bushveld parental magmas as constraints on the formation of the Merensky Reef in the Bushveld Complex, South Africa. In *Metallogeny of Basic and Ultrabasic Rocks* (eds. M. J. Gallagher, R. A. Ixer, C. R. Neary, and H. M. Prichard), pp. 183–198. London, Inst. Min. Metal.
- Hatton C. J. and von Gruenewaldt G. (1987) The geological setting and petrogenesis of the Bushveld chromitite layers. In *Evolution of Chromium Ore Fields* (ed. C. W. Stowe), pp. 109–143. New York, Van Nostrand Reinhold.
- Hooper P. R. (1988) The Columbia River Basalt. In *Continental Flood Basalts* (ed. J. D. MacDougall), pp. 1–33. Dordrecht, Kluwer Academic Publishers.
- Irvine T. N. and Sharpe M. R. (1986) Magma mixing and the origin of stratiform oxide ore zones in the Bushveld and Stillwater Complexes. In *Metallogeny of Basic and Ultrabasic Rocks*. (eds. M. J. Gallagher, R. A. Ixer, C. R. Neary, and H. M. Prichard), Lond. Inst. Min. Metal.
- Kinloch E. D. (1982) Regional trends in the platinum-group mineral-

- ogy of the Critical zone of the Bushveld Complex, South Africa. *Econ. Geol.* **77**, 1328–1347.
- Kinloch E. D. and Peyerl W. (1990) Platinum-group minerals in various rock types of the Merensky Reef: Genetic implications. *Econ. Geol.* **85**, 537–555.
- Kruger F. J. (1994) The Sr-isotope stratigraphy of the western Bushveld Complex. *S. Africa J. Geol.* **97**, 393–398.
- Kruger F. J. and Marsh J. S. (1982) Significance of $^{87}\text{Sr}/^{86}\text{Sr}$ ratios in the Merensky cyclic unit of the Bushveld Complex. *Nature* **298**, 53–55.
- Kruger F. J. and Corner B. (1987) The tectonic setting of the Bushveld Complex and other layered intrusions in southern Africa: Geophysical and isotopic evidence. Indaba on the tectonic setting of layered intrusives. *Geol. Soc. S. Africa*, 31–32.
- Lee C. A. and Butcher A. R. (1990) Cyclicity in the Sr isotope stratigraphy through the Merensky and Bastard Reef units, Atok section, eastern Bushveld Complex. *Econ. Geol.* **85**, 877–883.
- Liebenberg L. (1969) The sulphides in the layered sequence of the Bushveld Igneous Complex. In *Symposium on the Bushveld and Other Layered Intrusions* (eds. J. Visser and G. Von Gruenewaldt) *Geol. Soc. S. Africa Sp. Pub.* **1**, 108–207.
- Loebenstein J. R. (1984) Platinum-group minerals. *U.S. Bureau of Mines, Minerals Yearbook for 1983*, 685–695.
- Maier W. D. and Teigler B. (1995) A facies model for the western Bushveld Complex. *Econ. Geol.* **90**, 2343–2349.
- Mathez E. A., Agrinier P., and Hutchinson R. (1992) Hydrogen isotopic composition of the Merensky Reef and related rocks, Atok section, Bushveld Complex. *Eos* **73**, 372.
- McCandless T. E. and Ruiz J. (1991) Osmium isotopes and crustal sources for platinum-group mineralization in the Bushveld Complex, South Africa. *Geology* **19**, 1225–1228.
- McCandless T. E. and Ruiz, J. (1993) Rhenium-osmium evidence for regional mineralization in southwestern North America. *Science* **261**, 1282–1286.
- McCandless T. E., Ruiz J., and Adair B. I. (1994) Platinum group mineralization in the Bushveld Complex: A combined QEM-SEM and LA-ICPMS study. *Mineralogical Magazine* **58A**, 579–580.
- Merkle R. K. W. (1986) Estimation of recovery characteristics of the platinum-group minerals in some chromitite layers below the UG2 in the Bushveld Complex, South Africa. In *Metallogeny of Basic and Ultrabasic Rocks* (eds. M.J. Gallagher, R.A. Ixer, C.R. Neary, and H.M. Prichard), pp. 81–87. London, Inst. Min.
- Merkle R. K. W., von Gruenewaldt G., and Harney D. M. W. (1995) An evaluation of proposed platinum group element contents in the parental magmas of the Bushveld complex. *J. African Earth Sci.* **21**, 607–613.
- Morgan J. W. and Walker R. J. (1991) Isotopic determinations of rhenium and osmium in meteorites by using fusion, distillation and ion-exchange separations. *Anal. Chim. Acta.* **222**, 291–300.
- Mountain B. W. and Wood S. A. (1988) Solubility and transport of platinum-group elements in hydrothermal solutions; thermodynamic and physical chemical constraints. In *Geo-Platinum 87* (eds. H. M. Prichard, P. J. Potts, J. F. W. Bowles, and S. J. Cribb), pp. 57–82. New York, Elsevier.
- Naldrett A. J. and von Gruenewaldt G. (1988) The Upper Critical Zone of the Bushveld Complex and the origin of Merensky-type ores: A reply. *Econ. Geol.* **83**, 1085–1091.
- Naldrett A. J., Brugman G. E., and Wilson A. H. (1990) Models for the concentration of PGE in layered intrusions. *Can. Min.* **28**, 389–408.
- Nicholson D. M. and Mathez E. A. (1991) Petrogenesis of the Merensky Reef in the Rustenburg section of the Bushveld Complex. *Cont. Min. Pet.* **107**, 293–309.
- Peyerl W. (1982) The influence of the Driekop dunite pipe on the platinum-group mineralogy of the UG-2 chromitite in its vicinity. *Econ. Geol.* **77**, 1432–1438.
- Ravizza G. E. and Turekian K. K. (1989) Application of the ^{187}Re - ^{187}Os system to black shale geochronometry. *Geochim. Cosmochim. Acta* **53**, 3257–3262.
- Rice A. R. and Ealses H. V. (1995) The densities of Bushveld melts: Textural and hydrodynamic criteria. *Min. Pet.* **54**, 45–53.
- Ruiz J. R., McCandless T. E. and Adair B. I. (1992) Volatile effects on platinum-group minerals and osmium isotopes in Bushveld Igneous Complex, South Africa [abs]. *Eos*, **27**, 617.
- Saal A. E., Rudnick R. L., Ravizza G. E., and Hart S. R. (1998) Re-Os isotope evidence for the composition, formation and age of the lower continental crust. *Nature* **393**, 58–61.
- Schiffries C. M. (1982) The petrogenesis of a platiniferous dunite pipe in the Bushveld Complex: Infiltration metasomatism by a chloride solution. *Econ. Geol.* **82**, 1439–1453.
- Schiffries C. M. (1992) Crustal contamination of the Bushveld Complex. *Geol. Soc. Am. Abst. Prog.* **24**, A86.
- Schiffries C. M. and Rye D. M. (1989) Stable isotopic systematics of the Bushveld Complex: I. Constraints of magmatic processes in layered intrusions. *Am. J. Sci.* **289**, 841–873.
- Schiffries C. M. and Rye D. M. (1990) Stable isotopic systematics of the Bushveld Complex: II. Constraints on hydrothermal processes in layered intrusions. *Am. J. Sci.* **290**, 209–245.
- Schiffries C. M. and Skinner B. J. (1987) The Bushveld hydrothermal system: Field and petrologic evidence. *Am. J. Sci.* **287**, 566–595.
- Schreiber U. M., Eriksson P. G., and Snyman C. P. (1992) Mudrock geochemistry of the Proterozoic Pretoria Group, Transvaal Sequence (South Africa): Geological implications. *J. African Earth Sci.* **14**, 393–409.
- Scoon R. N. and Teigler B. (1994) Platinum-group element mineralization in the Critical Zone of the Western Bushveld Complex: I. Sulfide poor-chromitites below the UG-2. *Econ. Geol.* **89**, 1094–1121.
- Shannon M. C. and Agee C. B. (1998) Percolation of core melts at lower mantle conditions. *Science* **280**, 1059–1061.
- Sharpe M. R. (1985) Strontium isotope evidence for preserved density stratification in the main zone of the Bushveld Complex, South Africa. *Nature* **316**, 119–126.
- Sharpe M. R., Bahat D., von Gruenewaldt G. (1981) The concentric elliptical structure of the Bushveld complex and possible economic implications. *Geol. Soc. S. Africa Trans.* **84**, 239–244.
- Sharpe M. R., and Hulbert L. J. (1985) Ultramafic sills beneath the Bushveld Complex: Mobilized suspensions of early lower zone cumulates in a parental magma with boninitic affinities. *Econ. Geol.* **80**, 849–871.
- Shirey S. B. (1997) Re-Os isotopic compositions of Midcontinent Rift System picrites: Implications for plume-lithosphere interaction and enriched mantle sources. *Can. J. Earth Sci.* **34**, 489–503.
- Shirey S. B. and Walker R. J. (1995) Carius tube digestion for the measurement of Re and Os in geological samples. *Anal. Chem.*, **67**, 2136–2141.
- Smoliar M. I., Walker R. J., and Morgan J. W. (1996) Re-Os ages of group IIA, IIIA, IVA, and IVB iron from meteorites. *Science* **271**, 1099–1102.
- Stumpff E. F. (1986) Distribution, transport and concentration of platinum group elements. In *Metallogeny of Basic and Ultrabasic Rocks: The Zimbabwe Volume* (eds. M. J. Gallagher, R. A. Ixer, C. R. Neary, and J. M. Prichard), pp. 379–394. Institute of Mining and Metallurgy, London.
- Teigler B. (1990) Platinum group element distribution in the lower and middle group chromitites in the western Bushveld Complex. *Min. Pet.* **42**, 165–179.
- Teigler B. and Eales H. V. (1993) Correlation between chromite composition and PGE mineralization in the Critical Zone of the western Bushveld Complex. *Mineral. Dep.* **28**, 291–302.
- Teigler B., Eales H. V., and Scoon R. N. (1992) The cumulate succession in the Critical Zone of the Rustenburg Layered Suite at Brits, western Bushveld Complex. *S. Africa J. Geol.* **95**, 17–28.
- Turcotte D. L. and Schubert G. (1982) *Geodynamics*. N.Y. John Wiley & Sons. 450 p.
- Ulmer G. C., Grandstaff D. E., Hanson B., Gold D. P., and Deines P. (1990) Texture, crystallinity, ^{13}C data for graphite in mafic igneous plutons. *Eos* **71**, 661.
- Uken R. and Watkeys M. K. (1997) Diapirism initiated by the Bushveld Complex, South Africa. *Geology* **25**, 723–726.
- Vermaak C. F. (1970) The geology of the lower portion of the Bushveld Complex and its relationship to the floor rocks in the area west of the Pilanesberg, western Transvaal. *Geol. Soc. S. Africa Sp. Pub.* **1**, 242–262.
- Viljoen M. J., and Scoon R. N. (1985) The distribution and main geologic features of discordant bodies of iron-rich ultramafic pegmatite in the Bushveld Complex. *Econ. Geol.* **80**, 1109–1128.

- Völkering J., Walczyk T., and Heumann, K. G. (1991) Osmium isotope ratio determinations by negative thermal ionization mass spectrometry. *Int. J. Mass Spectrom. Ion Proc.* **105**, 147–149.
- von Gruenewaldt G., Sharpe M. R., and Hatton C. J. (1985) The Bushveld Complex: Introduction and review. *Econ. Geol.* **80**, 803–821.
- von Gruenewaldt G., Dicks D., De Wet J., and Horsch H. (1990) PGE mineralization in the Western Sector of the Eastern Bushveld Complex. *Min. Pet.* **42**, 71–95.
- Walraven F., Armstrong R. A., and Kruger F. (1990) A chronostratigraphic framework for the central Kaapvaal craton, the Bushveld, and the Vredefort structure. *Tectonophysics* **171**, 23–48.
- Walker R. J. (1988) Low-blank chemical separation of rhenium and osmium from gram quantities of silicate rock for measurement by resonance ionization mass spectrometry. *Anal. Chem.* **60**, 1231–1234.
- Walker R. J., Echeverria L. M., Shirey S. B., and Horan M. F. (1991) Re-Os isotopic constraints on the origin of volcanic rocks, Gorgona Island, Colombia: Os isotopic evidence for ancient heterogeneities in the mantle. *Cont. Min. Pet.* **107**, 150–162.
- Walker R. J., Morgan J. W., Czamanske G. K., Likhachev A. P., and Kuniylov, V. E. (1994) Re-Os isotopic evidence for a plume origin for Noril'sk-Talnakh ores and associated ultramafic rocks: Siberia, Russia. *Geochim. Cosmochim. Acta* **58**, 4179–4192.
- Walker R. J., Morgan J. W., and Horan M. F. (1995) Osmium-187 enrichments in some plumes: Evidence from core-mantle interaction? *Science* **269**, 819–822.
- Walker R. J., Morgan J. W., Hanski E. J., and Smolkin V. F. (1997a) Re-Os systematics of early Proterozoic ferropicrites, Pechenga Complex, NW Russia: Evidence for ancient ¹⁸⁷Os-enriched plumes. *Geochim. Cosmochim. Acta* **61**, 3145–3160.
- Walker R. J., Morgan J. W., Beary E. S., Smoliar M. I., Czamanske G. K., and Horan M. F. (1997b). Applications of the ¹⁹⁰Pt-¹⁸⁶Os isotope system to geochemistry and cosmochemistry. *Geochim. Cosmochim. Acta* **61**, 4799–4807.
- Willemsse J. (1969) The geology of the Bushveld igneous complex, the largest repository of magmatic ore deposits in the world. *Econ. Geol. Monograph* No. **4**, 1–22.